ISBN: 978-3-95450-184-7 doi:10.18429/JACoW-IPAC2018-THPML119

A TIME-OF-FLIGHT BASED ENERGY MEASUREMENT SYSTEM FOR THE LIGHT MEDICAL ACCELERATOR

F. Galizzi[1,2], M. Caldara[2], and A. Jeff[2]

[1]University of Bergamo, Via Galvani 2, 24044 Dalmine BG, Italy
[2]A.D.A.M. SA, Rue de Veyrot 11, 1217 Meyrin, Switzerland

Abstract

The LIGHT proton therapy facility [1] is the first compact Linac that will deliver proton beams up to 230 MeV for cancer treatment [2]. The proton beam is pulsed; pulses repetition rate can reach 200 Hz. LIGHT prototype is currently being commissioned by AVO/ADAM at CERN, while the first full installation is foreseen in 2019. Beam energy translates directly to range penetration in the body, so it is of the utmost importance to monitor it accurately especially for Linacs, since each beam pulse is directly transported to the patient. We present the implementation of a non-interceptive beam energy measurement system based on the Time-of-Flight technique. Unlike state of the art ToF systems this one has been designed to measure autonomously the mean energy of the beam with medical resolution (0.03 %) by processing as little as 1 µs of data providing the result within 1 to 2 ms over an energy range from 5 to 230 MeV. The first results for beams up to 7.5 MeV are shown.

TIME-OF-FLIGHT & PHASE PROBES

The Time-of-Flight is a non-destructive technique for the measurement of the energy of a beam of charged particles using phase probes. A phase probe (Fig. 1) mainly consists of a 50 Ω ring-shaped electrode on which is generated a voltage proportional to the derivative of the beam current passing through it. Probes are positioned along the beam pipe on a straight section without accelerating cavities in between, and the phase shift between their output signals is measured. This measure gives an estimation of the time taken by the beam to cover the distance between the two probes, so the beam velocity can be computed, and from that the energy:

$$T_x = \frac{\Delta\varphi_x}{2\pi}\cdot T_{\text{beam}}; \qquad \beta = \frac{L_x}{T_x}\cdot\frac{1}{c};$$
$$\gamma = \left(1-\beta^2\right)^{-\frac{1}{2}}; \qquad E = A\cdot E_0\cdot(\gamma-1); \quad (1)$$

where: $\Delta\varphi_x$ is the measured phase shift; T_{beam} is the repetition period of the beam bunches; T_x is the time taken by the particles to go from a probe to the other; L_x is the distance between the probes; c is the speed of light; A and E_0 are the mass number and the rest energy of the particle.

The energy measurement error is inversely proportional to the distance between probes, while the phase shift measurement range is directly proportional to probes distance and energy range; to measure a wide energy range a short-distance (e.g. 10 cm), low-resolution phase shift measurement is required to ensure the unambiguousness of a long-distance (e.g. 1 m), high-resolution phase shift measurement, gaining orders of magnitude (proportional to the distances ratio) for the energy measurement resolution. This led to the choice of a three-probes setup.

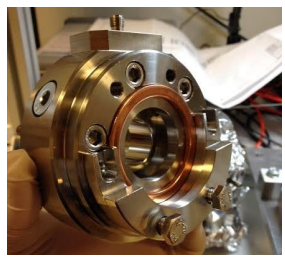

Figure 1: One of the three phase probes used in the ToF system for LIGHT.

MEASUREMENT UNCERTAINTY EVALUATION

Figure 2 represents the relation between the uncertainties on probes distance, measured phase shift and computed energy value. This is given by the following formula (derived from Eq. (1) by error propagation analysis):

$$\frac{\delta E}{E} \approx \frac{\beta^2\gamma^3}{\gamma-1}\cdot\sqrt{\left(\frac{\delta L}{L_x}\right)^2+\left(\frac{\delta\Delta\varphi}{2\pi}\cdot\frac{T_{\text{beam}}}{T_x}\right)^2}, \quad (2)$$

where δL is the uncertainty on the distance and $\delta\Delta\varphi$ is the uncertainty on the measured phase shift.

The measurement accuracy is inversely proportional to the energy, thus the worst case is for the largest measurable value (230 MeV, used for the plot). The detection accuracy limit (0.03 %, equivalent to a depth variation in the body of 0.2 mm) is a goal derived from medical requirements. The dashed lines highlights the current status for distance and phase shift accuracy.

Other components such as quadrupoles can be placed between the phase probes, provided that the trajectory excursion is small. This allows to increase the distance between the probes without increasing the beam pipe occupation.

SYSTEM DESCRIPTION

The Linac operates at 3 GHz, accelerating one bunch of particles every four periods, thus the output voltage signal

ISBN: 978-3-95450-184-7 doi:10.18429/JACoW-IPAC2018-THPML119

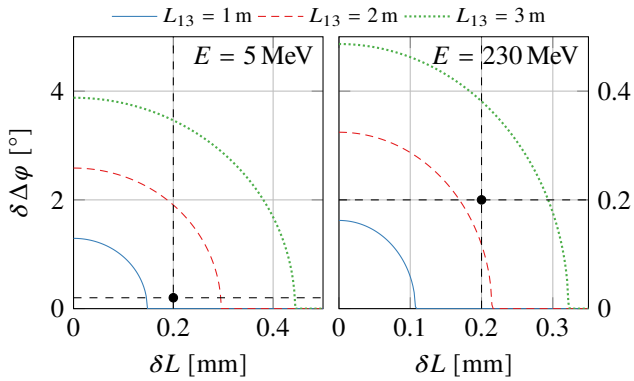

Figure 2: Relations between uncertainties to obtain $\frac{\delta E}{E}$ = 0.03 % at 5 MeV and 230 MeV, for different distances between the two furthest probes.

of the phase probes has a main component at 750 MHz; ToF is based on the processing of this harmonic only.

Each probe output signal is amplified by two amplifiers: a fixed-gain amplifier and a variable gain one, which allows to account for the broad intensity range of the beam and also for the variation of the probes transfer impedance which is inversely proportional to the beam energy. After amplification, the signals are down-mixed, to allow for an easier digitisation. This is performed by an acquisition board[1], which hosts ADCs and an FPGA, performing signals processing to extract the signals phases (and amplitudes).

The system also includes a calibration feature. Hardware-wise, this requires to add a voltage-controlled oscillator whose output is split and then injected into the electronic chains instead of the probes outputs. This allows to measure the phase shift between two channels outputs which is due only to manufacturing mismatch for the analog components. This allows to measure and cancel from the phase measurement the different phase offsets introduced by the three acquisition chains.

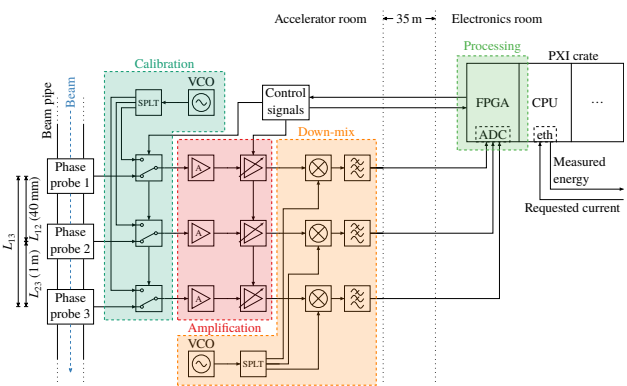

Figure 3: Hardware diagram of LIGHT's ToF system. Probes distances are for the current test stand.

[1] ADQ14DC-4C by Teledyne SP Devices.

SIGNAL PROCESSING

If the measured energy of a pulse differs by a certain extent from the value requested by the Treatment Planning System the next pulse must not be delivered to the patient. For this reason the processing has to be fast and real-time, in order to deterministically get a result in 1 to 2 ms. This led to the choice of an FPGA as processing unit, in accordance with modern ToF implementations [3].

LIGHT's beam is pulsed, meaning that beam bunches are grouped in pulses about 1 µs long. Pulses repetition rate can reach 200 Hz. Within a pulse the energy is fixed, but no assumption can be made about the energy change from pulse to pulse. This characteristic limits the temporal window over which signal features can be extracted, but allows to employ processing techniques which make use of a whole set of samples, as opposed to techniques which update estimations on a per-sample basis.

The analog down-mixing stage allows for an easier digitisation, but force to perform a frequency detection, because it's output frequency depends on the stability of the oscillator used to down-mix. This is performed by parabolic interpolation of the FFT peak of the signal, achieving a resolution of about 25 kHz (σ = 3.7 kHz) for a record of 1000 samples acquired at 1 Gsps.

The phase detection is performed by means of Digital Down Conversion (DDC), which is a digital implementation of the IQ down-conversion, over a whole pulse. Being performed on the whole pulse, the low-pass filtering required by the DDC can be substituted with the computation of the mean for I and Q, which is much simpler and computationally cheaper.

The achieved phase measurement resolution is about 0.05°. Given that also the calibration feature uses the same acquisition chain and processing, this is also the resolution of the phase offset measurement (in this case the accuracy could be increased by employing a longer time window or by averaging multiple measurements, but a proper strategy has not been established yet). The phase shift accuracy reported in Fig. 2 is thus an overestimate: in fact, $\Delta\varphi$ is computed as the difference of the phases of two signals, which in turn are computed as difference of the phase measurement on the beam pulse and the measured phase offset, so the accuracy can be computed to be $\sqrt{4} \cdot 0.05° = 0.1°$.

The small resolution allows to verify if the beam is well-controlled or not, as shown in Fig. 4: the plots on the left represents the measured phase shifts and the computed energy at 5 MeV after the commissioning of the employed cavities, while the plots on the right represents the same quantities at 7.5 MeV before the commissioning of the added cavity. Energy variations smaller than 1 keV can be detected.

$\Delta\varphi_{12}$ and $\Delta\varphi_{13}$ are the phase shifts measured over two different distances for the same pulse. If measurements were noiseless, for varying energy the two phase shifts would vary together in accordance with the formula (from Eq. (1)) $\Delta\varphi_{13} = \Delta\varphi_{12} \cdot \frac{L_{13}}{L_{12}}$: this behaviour would produce a straight line plot. The opposite would be having a fixed energy

ISBN: 978-3-95450-184-7 doi:10.18429/JACoW-IPAC2018-THPML119

with noisy measurements: this would produce a bi-variate gaussian plot with no correlation. It can be seen that in Fig. 4 the plots on the left are closer to the second case, while the plots on the right are closer to the first case.

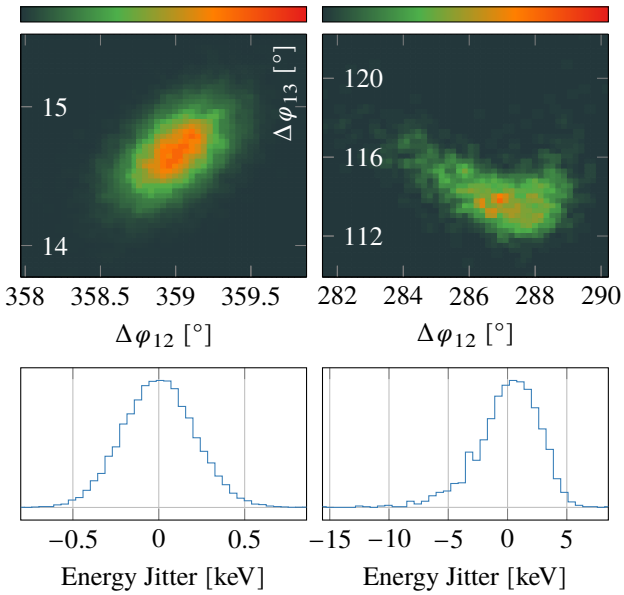

Figure 4: Measured phase shifts and computed energy. Left: at 5 MeV, after commissioning; right: at 7.5 MeV, before commissioning.

RESULTS

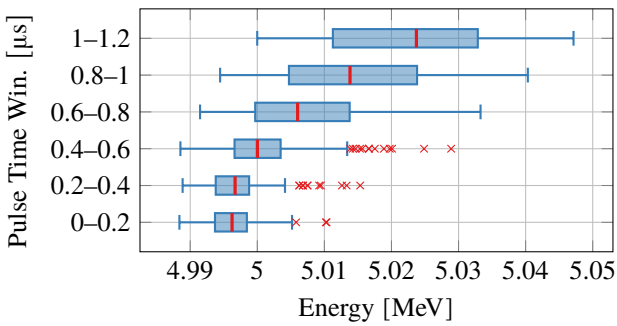

Figure 5: Beam pulse scan at 5 MeV (during early commissioning stage). Each box plot is the result of 200 measurements.

The developed system allows the detection of in-pulse dynamics. Figure 5 shows a measurement for a 1.2 µs beam pulse at 5 MeV. The first (lowest) box plot refers to measurements on the first 200 ns of the pulse, the second box plot refers to the following 200 ns of the pulse, and so on. It can be seen that going from the front to the back of the pulse not only the energy increases but also its jitter.

Figure 6 shows the results of the energy measurement for different levels of the RF field in the RFQ, which is measured with RF pickups. It can be noted that in the plot the particles energy is inversely proportional to the RFQ power: this can happen because the RFQ is built for a certain nominal power, so to deviate from the nominal conditions

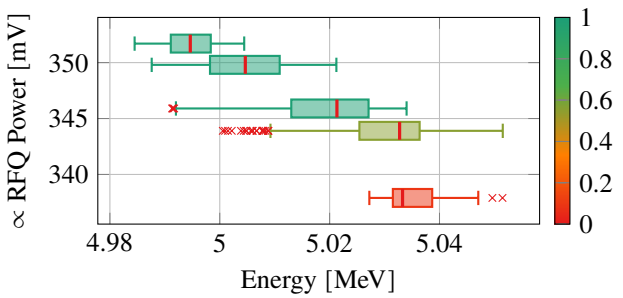

Figure 6: Beam energy measurements with varying RFQ power. Each box plot is the result of 700 measurements.

usually means that a smaller amount of power is transferred to the particles. The colour of each box plot is related to its statistical significance: changing the RFQ settings makes the beam unstable, producing invalid measurements. This kind of measurement can be exploited to speed up and improve the RFQ commissioning.

CONCLUSIONS & EVOLUTIONS

The ToF propotype presented in this paper is able to measure LIGHT beam energy for each pulse at 200 Hz. The measurement resolution can reach the 0.03 % goal, but it is in trade-off with the system compactness.

The system has to be extensively characterised for phase offsets and drifts, in order to establish the strategy to adopt for the phase offsets cancellation and thus improve the system accuracy. The system will also be cross-validated using a spectrometer.

The ToF system is presently installed in a BD test stand used for LIGHT commissioning, and will be used for the commissioning of all the cavities. In LIGHT final installation the ToF will be installed in the transfer line after the last accelerating module and it will be used to provide on-line beam energy measurements during treatments.

ACKNOWLEDGEMENTS

The authors would like to acknowledge Teledyne SP Devices for the provided hardware and for the technical support in the development of this system.

REFERENCES

[1] A Degiovanni, D Ungaro, and P Stabile, "LIGHT: A linear accelerator for proton therapy", *Proceedings of NAPAC2016*, pp. 1282–1286, 2016.

[2] U. Amaldi *et al.*, "Accelerators for hadrontherapy: From Lawrence cyclotrons to linacs", *Nuclear Instruments and Methods in Physics Research Section A: Accelerators, Spectrometers, Detectors and Associated Equipment*, vol. 620, no. 2, pp. 563–577, 2010. DOI: 10.1016/j.nima.2010.03.130.

[3] C. Jamet, W. Le Coz, C. Doutressoulles, T. André, and E. Swartvagher, "Phase and amplitude measurement for the SPIRAL2 Accelerator", *9th European Workshop on Beam Diagnostics and Instrumentation for Particle Accelators (DIPAC 2009)*, pp. 1–2, 2009.